Step-wise DNA methylation changes are linked to escape from defined proliferation barriers and mammary epithelial cell immortalization

Novak P[1,4], Jensen TJ[1,2], Garbe JC[3], Stampfer MR[3], Futscher BW[1,2].

[1]Arizona Cancer Center, The University of Arizona, Tucson, AZ 85724, USA

[2]Department of Pharmacology & Toxicology, College of Pharmacy, The University of Arizona, Tucson, AZ 85724, USA

[3]Life Sciences Division; Lawrence Berkeley National Laboratory, Berkeley, CA 94720 USA

[4]Biology Centre ASCR, v.v.i., Institute of Plant Molecular Biology, Ceske Budejovice, 37005, Czech Republic

*Corresponding Author
Bernard W. Futscher
Arizona Cancer Center
1515 N Campbell Ave
Tucson, AZ 85724
Email: (bfutscher@azcc.arizona.edu)
Phone: 520-626-4646
Fax: 520-626-4979

Running Title: Step-wise changes in DNA methylation precede immortalization

Key Words: DNA methylation, epigenetic, breast cancer, CpG island, silencing

Abstract

The timing and progression of DNA methylation changes during carcinogenesis are not completely understood. To develop a timeline of aberrant DNA methylation events during malignant transformation, we analyzed genome-wide DNA methylation patterns in an isogenic human mammary epithelial cell (HMEC) culture model of transformation. To acquire immortality and malignancy, the cultured finite lifespan HMEC must overcome two distinct proliferation barriers. The first barrier, stasis, is mediated by the retinoblastoma protein and can be overcome by loss of $p16^{INK4A}$ expression. HMEC that escape stasis and continue to proliferate become genomically unstable before encountering a second more stringent proliferation barrier, telomere dysfunction due to telomere attrition. Rare cells that acquire telomerase expression may escape this barrier, become immortal, and develop further malignant properties. Our analysis of HMEC transitioning from finite lifespan to malignantly transformed showed that aberrant DNA methylation changes occur in a stepwise fashion early in the transformation process. The first aberrant DNA methylation step coincides with overcoming stasis, and results in few to hundreds of changes, depending upon how stasis was overcome. A second step coincides with immortalization, and results in hundreds of additional DNA methylation changes, regardless of the immortalization pathway. A majority of these DNA methylation changes are also found in malignant breast cancer cells. These results show that large-scale epigenetic remodeling occurs in the earliest steps of mammary carcinogenesis, temporally links DNA methylation changes and overcoming cellular proliferation barriers, and provides a bank of potential epigenetic biomarkers that may prove useful in breast cancer risk assessment.

Introduction

Epigenetic dysfunction is a common and perhaps universal feature of human cancer. One facet of the epigenetic system that shows clear and dramatic differences between normal and cancer cells is DNA methylation. DNA hypermethylation generally occurs in CpG island gene promoters and is linked to transcriptional gene silencing, while DNA hypomethylation often occurs in repetitive elements, pericentromeric regions, and within the body of genes and has been linked to gene activation and chromosome instability. Studies into the biological consequences of hypo- and hypermethylation indicate that each plays a participative role in carcinogenesis (1, 2). While significant progress has been made in identifying aberrant methylation events that occur during carcinogenesis, the timing, origins, and consequences of these events remain incompletely understood.

We have used an HMEC model system that allows for assessment of changes in DNA methylation that occur at the earliest stages of multi-step human breast carcinogenesis. In this model, the transformation of normal finite lifespan HMEC to malignancy requires overcoming two distinct senescence-associated barriers to immortality (3). The first barrier, termed stasis or stress-induced senescence, is characterized by elevated levels of the cyclin-dependent kinase inhibitor $p16^{INK4A}$ (gene *CDKN2A*), which maintains the retinoblastoma protein in an active state (4). This barrier has been overcome or bypassed in cultured HMEC by various means, such as exposure to the chemical carcinogen benzo(a)pyrene, with the resultant post-stasis cells commonly exhibiting inactivation of *CDKN2A* by promoter hypermethylation or by gene mutation (4, 5). Loss of p16 expression due to silencing or mutation is also a frequent event during in vivo human breast cell transformation (6, 7). When grown in a serum-free medium, rare HMEC will “spontaneously” silence p16, generating a type of post-stasis HMEC population that has been called post-selection (4, 8). HMECs that have escaped stasis undergo further proliferation before encountering a second more stringent proliferation barrier resulting from critically shortened telomeres (3, 9). When approaching the telomere dysfunction barrier, HMEC exhibit increased chromosomal instability and a

DNA damage response. Rare cells that gain telomerase expression may escape this barrier, and acquire immortal potential; additional perturbations can confer malignant properties on the immortally transformed cells (5, 10-12).

This HMEC system has proven useful for identifying and reflecting the molecular events involved in early human breast tumorigenesis (3-5, 9, 13-15). For example, the hypermethylation of *CDKN2A* seen in post-stasis HMEC has also been documented in precancerous lesions and histologically normal breast tissue (15, 16). Currently it is not clear if focal DNA methylation changes, such as in p16, are rare events that accumulate independently and gradually over time or if these are examples of larger sets of DNA methylation changes that occur in groups - concurrently and at distinct points in the immortalization process. Genomic instability and telomere erosion, characteristic of pre-malignant, in situ breast lesions, is seen in the cultured HMEC at the telomere dysfunction barrier (3, 9, 13, 17). The potential contribution of epigenetic changes to telomerase reactivation and immortality is currently not known. To begin to address these questions we examined the DNA methylation profiles of cultured normal finite lifespan HMEC, isogenic derivatives induced to escape the stasis and/or telomere dysfunction barriers, established breast cancer cell lines, and human breast cancer specimens.

Our results demonstrate that aberrant DNA methylation patterns emerge at the earliest stages of HMEC transformation *in vitro*, in finite lifespan HMEC. Aberrant changes proceeded in a stepwise fashion, with each step temporally linked to escaping one of the two proliferation barriers. The first step of DNA methylation change occurs when stasis is overcome or bypassed, and results in few to hundreds of aberrant hyper- and hypomethylation events, depending upon the manner by which stasis was overcome. A majority of these events are found in breast cancer cells. The second step occurs in cells that have overcome the telomere dysfunction barrier and become immortal, and is associated with hundreds of aberrant methylation events, regardless of the manner of immortalization. A majority of these events are also found in breast cancer cells. Further methylation changes occur during malignant progression. These results

suggest that groups of DNA methylation changes can arise concurrently and in a step-wise fashion during early breast carcinogenesis.

Materials and Methods

Cell cultures. Organoids were obtained from reduction mammoplasty tissues as described (18). Finite lifespan pre-stasis HMEC from specimens 184 (batches D, E, F), 48 (batches RT, LT), and 240L (batch B), and post-selection HMEC 184 (batch B, telomere dysfunction arrest at ~passage 15), and 48 (batch RS, telomere dysfunction arrest at ~passage 23) were derived from tissue of women aged 21,16, and 19 respectively. Cells were initiated as organoids in primary culture in either serum-free MCDB 170 medium (MEGM, Clonetics Division of Lonza, Walkersville, MD) plus supplements (8), or serum-containing media MM (19) or M85 (composed of 50% MM and 50% supplemented MCDB 170 media) (Garbe et al, submitted). Post-selection HMEC were cultured in MCDB 170 as described (8, 18). The post-stasis 184Aa, 184Be, 184Ce cultures and the non-malignant immortal lines 184A1 and 184B5 were obtained from primary cultures of specimen 184 grown in MM, that had been exposed to the chemical carcinogen benzo(a)pyrene as described (5). 184A1-RF was obtained by retroviral transduction of the 184A1 line with the Raf-1 oncogene, and has gained anchorage-independent growth (AIG) (10). The p53-/- 184AA2 immortal line with AIG was obtained from 184Aa following insertional mutagenesis as described (20). The 184B5ME line with AIG was obtained by transfection of 184B5 with erbB2, and selection for anchorage-independent colonies. The post-stasis 184F-p16sh and 184D-p16sh cultures were obtained by retroviral transduction of pre-stasis HMEC cultures that were grown respectively in M85 and M87A+X (composed of 50% MM4 (19) and 50% supplemented MCDB 170 media plus 0.1% AlbuMax (Invitrogen) and 0.1 nM oxytocin (Bachem)). The non-malignant immortal 184ZNMY3 line was derived from post-selection 184B following retroviral transduction of ZNF217 and c-myc; 184ZNMY3-N with AIG was obtained following retroviral transduction of 184ZNMY3 with the mutated neu oncogene. Breast cancer cell lines were cultured as previously described (21).

Breast tumor specimens. Flash frozen specimens derived from normal or cancerous breast tissue were obtained from patients who underwent surgery for breast cancer, either lumpectomy or mastectomy, at the University Medical Center in Tucson, AZ., from 2003-2005. All patients signed surgical and clinical research consents for tissue

collection in accordance with the University of Arizona IRB and HIPAA regulations. At the time of surgery, a 1-3 cm section of the tumor was immediately snap frozen in liquid nitrogen and stored in our prospective breast tissue bank at -80 degree Celsius. From each tissue block, a series of 5 micron sections were cut and stained with hematoxylin and eosin (H&E) for pathological evaluation. All H&E slides were reviewed by two independent pathologists to determine the integrity of the tumor specimen. A partial molecular characterization of these samples have been reported on previously (21, 22). Supplementary Table 1 provides the pathological assessment of each specimen.

Nucleic acid isolation. RNA and DNA were isolated as previously described (21).

DNA methylation analysis by MassARRAY. Sodium bisulfite (NaBS) treated genomic DNA was prepared according to manufacturer's instructions (Zymo Research, Orange, CA). NaBS treated DNA (5 ng) was seeded into a region specific PCR reaction incorporating a T7 RNA polymerase sequence as described by the manufacturer (Sequenom, San Diego, CA). Resultant PCR product was then subjected to *in vitro* transcription and RNase A cleavage using the MassCLEAVE T-only kit, spotted onto a Spectro CHIP array, and analyzed using the MassARRAY Compact System MALDI-TOF mass spectrometer (Sequenom, San Diego, CA). Each NaBS treated DNA sample was processed in two independent experiments. Data were analyzed using EpiTyper software (Sequenom, San Diego, CA) as described (22, 23). Primer sequences were designed using EpiDesigner (www.epidesigner.com). Primer sequences are available upon request.

Methyl DNA immunoprecipitation microarrays and data analysis. Methylated fraction of DNA was obtained by immunoprecipitation as described (21). Input and immunoprecipitated DNA were amplified, labeled and analyzed on Human Promoter arrays as described (24). All microarray data were processed in R programming environment using *Limma* package was used and differentially methylated elements were identified using statistical approaches as described previously (25). To control for false discovery rate, a multiple testing correction was performed according to the

methods described (24). A list of differentially methylated elements is provided in Supplementary Table 2. A region was considered differentially methylated if the adjusted p value was lower than 0.05 and there was at least a 1.25 fold change in methylcytosine immunoprecipitated DNA versus input DNA ratio relative to pre-stasis HMEC. The magnitude of the microarray methylation ratio was directly correlated with the degree of methylation, as determined by MassARRAY (Supplementary Figure 1). All raw and normalized microarray data with detailed protocols are available in the ArrayExpress database; accession E-MEXP-1889 (www.ebi.ac.uk/arrayexpress). The number of and samples analyzed by DNA methylation microarray are provided in Supplementary Table 3. Gene ontology terms over-representation testing was performed using GOstats package (26). Overlapping probabilities of DMR sets were calculated using a hypergeometric test (27).

Results

DNA methylation changes during transformation. Figure 1 shows the cells analyzed in this study, their relative position with respect to proliferation barriers, the predicted corresponding *in vivo* correlates (3, 9, 13), the timing and accumulation of genetic abnormalities (9, 13, 28-30), and finally the timing and accumulation of DNA methylation changes determined in this study. The DNA methylation state of HMEC at different stages in the transformation from normal finite pre-stasis to immortal with AIG, as well as of malignant breast cancer cell lines, was analyzed using a 13,500 element human gene promoter microarray (24); arrows in the bottom panel indicate when cells were examined.

The first step of DNA methylation change occurs when stasis is overcome or bypassed and post-stasis HMEC emerge (Figure 2A). When pre-stasis HMEC are compared to post-selection HMEC (48RS and 184B) that overcame stasis associated with silencing of p16 following culture in a stress-inducing serum-free medium (8), 191 differentially methylated regions (DMRs) were identified, in addition to the previously described *CDKN2A* methylation (4). This number represents approximately 2% of all promoters analyzed on this microarray. In contrast, HMEC that become post-stasis following exposure to the mutagen and complete carcinogen benzo(a)pyrene (184Aa, 184Be, 184Ce) (5, 31) exhibited only 10 DMR when compared to pre-stasis HMEC. Although this is a very small number of elements that could represent false discoveries or stochastic events, it appears that at least a few are valid and relevant, such as the *HOXA* gene cluster, since this is a common target among all these post-stasis HMEC samples, as well as clinical disease. Supplementary Figure 2 shows high resolution methylation analysis that confirms aberrant methylation of the HOXA4 locus in the benzo(a)pyrene treated HMEC. In contrast, HMEC that became post-stasis following transduction with p16 shRNA (184F-p16sh, 184D-p16sh) accumulated only 5 DMRs, and did not show changes in the HOXA gene cluster. These results suggest that different levels of DNA methylation changes may be associated with HMEC that overcome the stasis proliferation barrier via different genetic or epigenetic mechanisms.

Considering that the number of aberrantly methylated genes in cancer has been estimated to be between several hundreds to low thousands (1, 22, 32), and the large number of DMRs seen in the post-selection HMEC, the transition through the stasis proliferation barrier may represent a critical epigenetic event in some pathways of carcinogenesis.

The second step of DNA methylation change occurs when telomere dysfunction is overcome and cells become immortal (Figure 2A). This second stepwise increase in DNA methylation changes produced hundreds of new DMRs, regardless of how telomere dysfunction or stasis was overcome. Breast cancer cell lines derived from malignant tumors displayed the greatest number of aberrant DNA methylation changes. Taken together, these results are consistent with progressive, stepwise increases in aberrant DNA methylation during the transformation process.

To further address whether aberrant DNA methylation progresses in a gradual or step-wise fashion in the earliest stages of breast carcinogenesis, we examined multiple early and late passage pre-stasis and post-selection HMEC, including cell passages in telomere dysfunction, that are known to have genomic instability (9) (Figure 2B). A comparison of the DNA methylation patterns of early and late passage pre-stasis HMEC revealed no DMRs. Similarly, no additional DMRs were detected when early passage post-selection HMEC were compared to those at telomere dysfunction. These results showed that there is not a gradual progression or increase in the number of DMRs between proliferative barriers, but rather new DMRs emerge in cells that overcame stasis or telomere dysfunction. Such step-wise changes are demonstrated on Figure 2B which shows the methylation status of post-stasis specific DMRs and breast cancer cell line specific DMRs at various stages of transformation. The abrupt increase in DNA methylation changes in post-stasis and immortal cells show the breakpoints of epigenetic reprogramming.

DNA methylation changes seen during *in vitro* transformation model the changes seen in *in vivo* carcinogenesis. If the DNA methylation changes found in post-stasis

HMEC and immortal HMEC cell lines are relevant to malignant transformation, then the identified methylation changes should resemble those seen in malignant breast cancer cell lines. Figure 2C is a Venn diagram relating the DMR found in post-stasis and immortal HMEC, and genetically distinct breast cancer cell lines. Of the 203 DMRs found in post-stasis HMEC populations, 136 DMRs (67%) are also aberrantly methylated in breast cancer cell lines (overlapping probability p value < 2.2 x10e-16). Furthermore, of the 484 DMRs identified in the immortalized HMEC lines, 327 (68%) are also found in breast cancer cell lines (p value < 2.2 x10e-16). Supplementary Figure 3 shows the overlap and differences in DMRs between immortal cell lines that bypassed this proliferation barrier by different mechanisms. These data indicate that a significant overlap exists between the targets of aberrant DNA methylation in breast cancer cells and the targets of aberrant DNA methylation in the pre-malignant stages represented by the HMEC model.

Step-wise changes in DNA methylation in specific gene clusters at defined proliferation barriers. To further examine the timing of specific methylation events, two gene clusters known to undergo aberrant methylation during breast carcinogenesis were examined in the gene promoter microarrays. Previous studies have shown frequent hypermethylation and silencing of the *HOXA* and *PCDH* gene family clusters in breast cancer (21, 22). Our data indicate that a prevalence of aberrantly methylated HOXA genes is also seen in both post-stasis and immortal HMEC. Detailed exploration of the *HOXA* genomic region showed that silencing of the whole cluster can originate early in breast carcinogenesis (Figure 3). Early DNA methylation changes occur in *HOXA3*, *HOXA4*, *HOXA9*, *HOXA10* and *HOXA13* genes in the post-selection HMEC. Interestingly, the *HOXA* cluster is also one of the few regions where DMRs emerged in post-stasis cells that bypassed stasis following exposure to benzo(a)pyrene; however, the *HOXA* cluster was not targeted in HMEC that bypassed stasis via silencing of p16 by shRNA. Further progression in aberrant DNA methylation occurs in the HOXA gene cluster in the immortal HMEC cell lines that overcame the telomere dysfunction barrier. Continued malignant progression is ultimately associated with aberrant DNA hypermethylation of the whole gene cluster as seen in the breast cancer lines.

A similar progression in aberrant DNA methylation occurs in another genomic region, the *PCDH* gene family cluster. However, detailed exploration of the *PCDH* genomic region showed that in this cluster, most changes are observed in the transition from post-stasis to immortal HMEC (Supplementary figure 4). Whereas almost no changes were seen in the post-stasis HMEC, the non-malignant immortal cell lines already displayed most of the changes seen in the breast tumor lines. These results clearly illustrate the step-wise nature of the DNA methylation changes in association with overcoming the proliferation barriers to immortality.

High Resolution Confirmation of DNA Methylation Changes. To confirm the methylation microarray data and extend our model, we analyzed the methylation status of post-stasis specific DMRs in pre-stasis, post-stasis, and immortalized HMEC, a set of primary breast tumors, and breast epithelial organoids using MassARRAY (Figure 4, Supplementary Figure 3). Results obtained confirmed the microarray data and extended them by showing that the DNA methylation changes seen in the *in vitro* model of post-stasis HMEC can also be found in primary breast tumors, but are not present in the normal epithelial organoids used to establish the HMEC system (18). In addition to the inappropriate methylation of *CDKN2A* as reported in focal aggregates of histologically normal mammary epithelia(15, 16) and in atypical ductal hyperplasia (ADH) (33), we also found the promoter region of *PGR* to be inappropriately methylated in post-stasis cells, similar to findings in ADH (34). Overall, these results indicate that post-stasis HMEC are a relevant model of early epigenetic changes in breast carcinogenesis, and that the hundreds of DMRs discovered may serve as potential markers of pre-malignant breast lesions.

Gene Ontology of DNA Methylation Targeted Promoters. To evaluate the potential functional importance of the DNA methylation changes, we analyzed the ontology of the genes where the promoters were targeted for changes in DNA methylation, and we found several overrepresented groups of genes (Supplementary figure 5). A significant number of genes involved in the extracellular matrix and the extracellular region were

hypermethylated in post-stasis cells, consistent with published gene expression data that showed differential expression of extracellular matrix and cell-cell communication genes between pre-stasis and post-stasis HMEC (14). Another noteworthy group of affected genes that are hypermethylated in both post-stasis and breast cancer cell lines is the gene ontology group related to adhesion and the plasma membrane. This gene ontology analysis revealed groups of genes targeted by aberrant DNA methylation in premalignant mammary epithelial that are also found to be dysregulated in breast cancer, suggesting that epigenetic changes important to the malignant phenotype may occur early in the multistep process of malignant transformation and prior to immortalization.

Discussion

In this report, we have shown that the transition of cultured HMEC from normal finite lifespan to immortality is associated with a step-wise progression of DNA methylation changes, and that these steps are coincident with passage through the defined epithelial cell proliferation barriers of stasis and telomere dysfunction. HMEC that emerged from these proliferation barriers acquired hundreds of DNA methylation changes compared to cells examined just prior to the proliferation barrier. In contrast, no changes in DNA methylation were observed between early and late passage cell populations that preceded the proliferation barriers. These results suggest a direct mechanistic link between epigenetic dysfunction and escape from senescence barriers thought to function as tumor suppressor mechanisms. Importantly, a majority of the two-step DNA methylation changes identified using this HMEC system are also seen in both breast cancer cell lines and tumor specimens. Since these methylation changes occurred at the earliest stages of transformation, in still finite lifespan HMEC populations, our results suggest that numerous aberrant methylation changes may be present in pre-malignant lesions of breast cancer. Indeed, several genes previously shown to have hypermethylated promoters in histologically normal mammary epithelia and premalignant stages of breast carcinogenesis were also identified in this study, including the *CDKN2A* and *PGR* promoters (15, 16, 33-37).

Gene Ontology analysis of the promoters targeted by DNA methylation showed that genes involved in the biological process of multicellular organismal development were overrepresented in both post-stasis cells and cancer cell lines, suggesting these targets may participate in the initiation and maintenance of the malignant phenotype (Supplementary Figure 5). *HOXA* genes are prominent in this list and are represented by *HOXA2*, *HOXA4*, *HOXA9*, *HOXA10*, *HOXA11*, and *HOXA13*. The disruption of these transcriptional regulators, which are involved in control of cell identity, are logical genes to be targeted in the malignant transformation process, and the consequences of their dysregulation are likely manifest through changes in the expression of *HOXA* target genes. The fact that aberrant DNA methylation and transcriptional dysregulation of the *HOXA* gene cluster is seen in a variety of human tumor types suggests that these

events play a critical role in human carcinogenesis (21, 38-40). Based on this information we speculate that *HOXA* genes are critical targets in the epigenetic initiation of malignant transformation.

The *HOXA* genes also represent a gene family cluster that frequently undergoes Long Range Epigenetic Silencing (LRES) in invasive breast cancer (21, 22, 41, 42). Interestingly, the *PCDH* gene family clusters (α, β, γ) on chromosome 5, another known target of LRES epigenetic silencing in invasive breast cancer, are also represented in the early steps of our *in vitro* model of transformation (22). The increased DNA methylation observed in these two known LRES targets provide evidence that 1) LRES is initiated early in mammary epithelial cell transformation, 2) LRES likely initiates in a step-wise fashion, similar to the focal events observed in this study, and 3) the *in vitro* HMEC system is an accurate reflection of the clinical disease. Taken together these results suggest that the post-stasis specific and the immortalization specific DMRs identified in this study may serve as potential markers of pre-malignant events in breast carcinogenesis. The specific DNA methylation changes identified in this study can potentially provide a bank of epigenetic biomarkers for assessing breast cancer risk, and allow for the analysis of multiple post-stasis and immortalization specific DNA methylation changes that when combined with additional types of genomic data (e.g. SNPs, gene expression) will help develop increasingly robust risk assessment models.

We examined cells that escaped stasis by three distinct means, exposure to the chemical carcinogen benzo(a)pyrene, growth in a stress-inducing serum-free medium, and direct inactivation of p16 by p16shRNA; the first two methods generated clonal post-stasis populations. The extent of DNA methylation changes at this step varied greatly, depending upon the manner by which the HMEC had become post-stasis. Post-selection HMEC displayed DNA methylation changes at hundreds of gene promoters, including *CDKN2A*, while HMEC that bypassed stasis following benzo(a)pyrene exposure or direct genetic inactivation of p16 showed few changes. These results suggest that different pathways to post-stasis produce different epigenetic signatures. Notably, however, the DNA methylation state of the *HOXA* gene cluster is

perturbed in all post-selection and benzo(a)pyrene exposed post-stasis cultures, regardless of pathway taken. These results suggest that within the emerging transformation-associated epigenetic signatures, there may be common critical epigenetic targets affected by the distinct paths and etiologies of breast cell transformation. The epigenetic aberrations that are common to the different pathways may play a critical role in driving the transformation process forward – the early deregulation of the *HOX* gene family clusters, which are decisively linked to human carcinogenesis, are one clear example that is consistent with this possibility (21, 39, 40). In contrast, the epigenetic aberrations that are specific to particular pathways to post-stasis and therefore occur at this earliest stage of transformation may allow for the emergence of distinct phenotypes if these cells pass to immortality and malignancy.

Although the stasis proliferation barrier could be bypassed with minimal epigenetic changes, all the immortalized lines examined acquired hundreds of additional DNA methylation changes, regardless of how they became post-stasis or immortal. These results suggest that DNA methylation changes may be necessary to achieve immortality. The role of epigenetic control in telomerase reactivation remains controversial and incompletely understood (43, 44). To address the potential role of DNA methylation in the control of *hTERT* in this HMEC model system, future studies will perform high resolution epigenetic analyses of the *hTERT* region. It is also possible that critical epigenetic changes within the multitude of genes affected during the transition to immortality are important and participate in telomerase reactivation.

Taken together, these results indicate that epigenetic alterations in DNA methylation found in breast cancer cells *in vivo* may arise during the earliest stages of HMEC transformation, prior to and coincident with attainment of immortality. Thus full understanding of the timing and nature of epigenetic alterations in early breast carcinogenesis will require examination of cells prior to attaining immortality. While non-malignant immortalized lines such as 184A1, 184B5, and MCF10A can be useful starting points for studying epigenetic events involved in the progression to invasive malignancy, they already possess many of the epigenetic aberrations found in breast

cancers. Similarly, the post-selection HMEC, although finite, also possess many epigenetic changes found in breast cancer cells. This finding is of particular note since post-selection HMEC are sold commercially as normal primary cells.

Overall, these results support an epigenetic progenitor model whereby genome-wide DNA methylation changes occur early, in a stepwise fashion, may precede genetic mutations, and allow for an inappropriate proliferation and expansion of epigenetically comprised progenitor cells (45). The large number of genes affected by aberrant DNA methylation provides a foundation for phenotypic variability in cells that transform to immortality and malignancy, and may be an important force that drives the significant biological heterogeneity seen in the clinical disease. The DNA methylation changes identified in this HMEC model system can potentially provide a bank of epigenetic biomarkers for assessing breast cancer risk in pre-malignant lesions, and provide targets for therapeutic interventions.

Acknowledgments
Received 12/31/08; revised 3/27/09; accepted 4/20/09; published OnlineFirst 6/9/09.
Grant support: Grants R01CA65662 and R33CA091351 (B.W. Futscher); center grants P30ES06694 and P30CA023074 and the BIO5 Interdisciplinary Biotechnology Center at the University of Arizona (Genomics Shared Service); training grants ES007091 and CA09213(T. J. Jensen); and NIH grant U54 CA112970, Department of Defense grant BCRP BC060444, and Office of Energy Research, Office of Health and Biological Research, U.S. Department of Energy contract DE-AC02-05CH11231 (J.C. Garbe and M.R. Stampfer).
The costs of publication of this article were defrayed in part by the payment of page charges. This article must therefore be hereby marked advertisement in accordance with 18 U.S.C. Section 1734 solely to indicate this fact. We thank Jose Munoz-Rodriguez (University of Arizona) and Batul Merchant (Lawrence Berkeley National Laboratory) for outstanding technical support.

References

1. Jones PA, Baylin SB. The epigenomics of cancer. Cell 2007;128(4):683-92.
2. Jones PA, Laird PW. Cancer epigenetics comes of age. Nat Genet 1999;21(2):163-7.
3. Garbe JC, Holst CR, Bassett E, Tlsty T, Stampfer MR. Inactivation of p53 function in cultured human mammary epithelial cells turns the telomere-length dependent senescence barrier from agonescence into crisis. Cell Cycle 2007;6(15):1927-36.
4. Brenner AJ, Stampfer MR, Aldaz CM. Increased p16 expression with first senescence arrest in human mammary epithelial cells and extended growth capacity with p16 inactivation. Oncogene 1998;17(2):199-205.
5. Stampfer MR, Bartley JC. Induction of transformation and continuous cell lines from normal human mammary epithelial cells after exposure to benzo[a]pyrene. Proc Natl Acad Sci U S A 1985;82(8):2394-8.
6. Geradts J, Wilson PA. High frequency of aberrant p16(INK4A) expression in human breast cancer. Am J Pathol 1996;149(1):15-20.
7. Baylin SB, Herman JG, Graff JR, Vertino PM, Issa JP. Alterations in DNA methylation: a fundamental aspect of neoplasia. Adv Cancer Res 1998;72:141-96.
8. Hammond SL, Ham RG, Stampfer MR. Serum-free growth of human mammary epithelial cells: rapid clonal growth in defined medium and extended serial passage with pituitary extract. Proc Natl Acad Sci U S A 1984;81(17):5435-9.
9. Romanov SR, Kozakiewicz BK, Holst CR, Stampfer MR, Haupt LM, Tlsty TD. Normal human mammary epithelial cells spontaneously escape senescence and acquire genomic changes. Nature 2001;409(6820):633-7.
10. Olsen CL, Gardie B, Yaswen P, Stampfer MR. Raf-1-induced growth arrest in human mammary epithelial cells is p16-independent and is overcome in immortal cells during conversion. Oncogene 2002;21(41):6328-39.
11. Stampfer MR, Yaswen P. Human epithelial cell immortalization as a step in carcinogenesis. Cancer Lett 2003;194(2):199-208.
12. Clark R, Stampfer MR, Milley R, *et al.* Transformation of human mammary epithelial cells by oncogenic retroviruses. Cancer Res 1988;48(16):4689-94.
13. Chin K, de Solorzano CO, Knowles D, *et al.* In situ analyses of genome instability in breast cancer. Nat Genet 2004;36(9):984-8.
14. Li Y, Pan J, Li JL, *et al.* Transcriptional changes associated with breast cancer occur as normal human mammary epithelial cells overcome senescence barriers and become immortalized. Mol Cancer 2007;6:7.
15. Holst CR, Nuovo GJ, Esteller M, *et al.* Methylation of p16(INK4a) promoters occurs in vivo in histologically normal human mammary epithelia. Cancer Res 2003;63(7):1596-601.
16. Bean GR, Bryson AD, Pilie PG, *et al.* Morphologically normal-appearing mammary epithelial cells obtained from high-risk women exhibit methylation silencing of INK4a/ARF. Clin Cancer Res 2007;13(22 Pt 1):6834-41.
17. Stampfer MR, Bodnar A, Garbe J, *et al.* Gradual phenotypic conversion associated with immortalization of cultured human mammary epithelial cells. Mol Biol Cell 1997;8(12):2391-405.

18. Stampfer MR. Isolation and growth of human mammary epithelial cells. J Tissue Culture Methods 1985;9:107-16.
19. Stampfer MR. Cholera toxin stimulation of human mammary epithelial cells in culture. In Vitro 1982;18(6):531-7.
20. Stampfer MR, Garbe J, Nijjar T, Wigington D, Swisshelm K, Yaswen P. Loss of p53 function accelerates acquisition of telomerase activity in indefinite lifespan human mammary epithelial cell lines. Oncogene 2003;22(34):5238-51.
21. Novak P, Jensen T, Oshiro MM, *et al.* Epigenetic inactivation of the HOXA gene cluster in breast cancer. Cancer Res 2006;66(22):10664-70.
22. Novak P, Jensen T, Oshiro MM, Watts GS, Kim CJ, Futscher BW. Agglomerative epigenetic aberrations are a common event in human breast cancer. Cancer Res 2008;68(20):8616-25.
23. Coolen MW, Statham AL, Gardiner-Garden M, Clark SJ. Genomic profiling of CpG methylation and allelic specificity using quantitative high-throughput mass spectrometry: critical evaluation and improvements. Nucleic Acids Res 2007;35(18):e119.
24. Jensen TJ, Novak P, Eblin KE, Gandolfi AJ, Futscher BW. Epigenetic remodeling during arsenical-induced malignant transformation. Carcinogenesis 2008;29(8):1500-8.
25. Smyth GK. Linear models and empirical bayes methods for assessing differential expression in microarray experiments. Stat Appl Genet Mol Biol 2004;3:Article3.
26. Falcon S, Gentleman R. Using GOstats to test gene lists for GO term association. Bioinformatics 2007;23(2):257-8.
27. Fury W, Batliwalla F, Gregersen PK, Li W. Overlapping probabilities of top ranking gene lists, hypergeometric distribution, and stringency of gene selection criterion. Conf Proc IEEE Eng Med Biol Soc 2006;1:5531-4.
28. Kuukasjarvi T, Karhu R, Tanner M, *et al.* Genetic heterogeneity and clonal evolution underlying development of asynchronous metastasis in human breast cancer. Cancer Res 1997;57(8):1597-604.
29. Nishizaki T, DeVries S, Chew K, *et al.* Genetic alterations in primary breast cancers and their metastases: direct comparison using modified comparative genomic hybridization. Genes Chromosomes Cancer 1997;19(4):267-72.
30. Walen KH, Stampfer MR. Chromosome analyses of human mammary epithelial cells at stages of chemical-induced transformation progression to immortality. Cancer Genet Cytogenet 1989;37(2):249-61.
31. Stampfer MR, Bartley JC. Human mammary epithelial cells in culture: differentiation and transformation. Cancer Treat Res 1988;40:1-24.
32. Costello JF, Fruhwald MC, Smiraglia DJ, *et al.* Aberrant CpG-island methylation has non-random and tumour-type-specific patterns. Nat Genet 2000;24(2):132-8.
33. Liu T, Niu Y, Feng Y, *et al.* Methylation of CpG islands of p16(INK4a) and cyclinD1 overexpression associated with progression of intraductal proliferative lesions of the breast. Hum Pathol 2008.
34. Melnikov AA, Scholtens DM, Wiley EL, Khan SA, Levenson VV. Array-based multiplex analysis of DNA methylation in breast cancer tissues. J Mol Diagn 2008;10(1):93-101.
35. Lee JS. GSTP1 promoter hypermethylation is an early event in breast carcinogenesis. Virchows Arch 2007;450(6):637-42.

36. Umbricht CB, Evron E, Gabrielson E, Ferguson A, Marks J, Sukumar S. Hypermethylation of 14-3-3 sigma (stratifin) is an early event in breast cancer. Oncogene 2001;20(26):3348-53.
37. Futscher BW, O'Meara MM, Kim CJ, *et al.* Aberrant methylation of the maspin promoter is an early event in human breast cancer. Neoplasia 2004;6(4):380-9.
38. Ordway JM, Bedell JA, Citek RW, *et al.* Comprehensive DNA methylation profiling in a human cancer genome identifies novel epigenetic targets. Carcinogenesis 2006;27(12):2409-23.
39. Rauch T, Wang Z, Zhang X, *et al.* Homeobox gene methylation in lung cancer studied by genome-wide analysis with a microarray-based methylated CpG island recovery assay. Proc Natl Acad Sci U S A 2007;104(13):5527-32.
40. Strathdee G, Holyoake TL, Sim A, *et al.* Inactivation of HOXA genes by hypermethylation in myeloid and lymphoid malignancy is frequent and associated with poor prognosis. Clin Cancer Res 2007;13(17):5048-55.
41. Frigola J, Song J, Stirzaker C, Hinshelwood RA, Peinado MA, Clark SJ. Epigenetic remodeling in colorectal cancer results in coordinate gene suppression across an entire chromosome band. Nat Genet 2006;38(5):540-9.
42. Hitchins MP, Lin VA, Buckle A, *et al.* Epigenetic inactivation of a cluster of genes flanking MLH1 in microsatellite-unstable colorectal cancer. Cancer Res 2007;67(19):9107-16.
43. Zinn RL, Pruitt K, Eguchi S, Baylin SB, Herman JG. hTERT is expressed in cancer cell lines despite promoter DNA methylation by preservation of unmethylated DNA and active chromatin around the transcription start site. Cancer Res 2007;67(1):194-201.
44. Renaud S, Loukinov D, Abdullaev Z, *et al.* Dual role of DNA methylation inside and outside of CTCF-binding regions in the transcriptional regulation of the telomerase hTERT gene. Nucleic Acids Res 2007;35(4):1245-56.
45. Feinberg AP, Ohlsson R, Henikoff S. The epigenetic progenitor origin of human cancer. Nat Rev Genet 2006;7(1):21-33.

Figure Legends

Figure 1. Schematic representation of breast cancer progression and the timing of the underlying genomic and DNA methylation changes. Connection between the *in vitro* system and *in vivo* progression is based on the previously published data describing genomic changes (9, 13, 30). The uppermost panel shows the temporal position of the two epithelial cell proliferation barriers of stasis and telomere dysfunction, and divides the timeline into pre-stasis, post-stasis, and immortal epithelial cells. The next panel shows the corresponding cell culture models used in this study. The treatment or genetic manipulation used is labeled in red. Cell models are described in detail in Materials and Methods. The lower panels show the *in vivo* correlates of the HMEC system, followed by the timeline of previously described genomic dysfunction in HMEC, and finally the timeline of DNA methylation changes identified and described in this study. Arrows on the DNA methylation changes curve shows the time points analyzed for DNA methylation state.

Figure 2. Stepwise progression of DNA methylation changes in an HMEC model of acquired immortality. (**a**) Total number of DNA hyper- and hypomethylation changes in groups of post-stasis HMEC, indefinite lifespan HMEC, and breast cancer cell lines when compared to pre-stasis HMEC. A total of 11,328 of gene promoter regions were analyzed. For purposes of statistical testing, some cell cultures were treated as one group (biological replicate) and each of these groups is represented by one bar. (**b**) Stepwise progression of DNA methylation in post-stasis specific DMRs and cancer cell line specific DMRs. DNA methylation on the *y-axis* is based on the normalized microarray data and corresponds to the log2 ratio of methylcytosine immunoprecipitated DNA versus input DNA. The passage number of each HMEC culture analyzed is in parenthesis. Only the hypermethylated DMRs are shown. Samples are color coded with blue boxes corresponding to pre-stasis cells, green to post-stasis cells, and red to immortalized cell lines including breast cancer cell lines. (**c**) Venn diagram showing common and unique DMRs between post stasis HMEC, immortalized HMEC, and

breast cancer cell lines. The post-stasis category represents DMRs detected in any post stasis HMEC group, the indefinite lifespan category represents DMRs detected in at least two of the immortal HMEC lines and the breast cancer cell line category represents DMRs found in at least two of the three breast cancer cell lines analyzed. The significance of overlap between post-stasis HMEC and breast cancer cell lines and between immortalized HMEC and breast cancer cell lines was calculated using a hypergeometric test.

Figure 3. Progression of DNA methylation in the *HOXA* gene family cluster from finite lifespan HMEC to malignantly transformed breast cancer cells. The top portion of the figure shows a map of the RefSeq genes of the *HOXA* cluster taken from UCSC Genome Browser (http://genome.ucsc.edu), followed by the location of CpG islands. The DNA methylation state of the *HOXA* gene family cluster based on the microarray data obtained from the various HMEC stages and breast cancer cell lines is shown in a heat map format and presented in physical scale along the *HOXA* cluster. Green represents hypomethylated, red hypermethylated sites. Nucleotide position along chromosome 7 is shown below the heat map.

Figure 4. Detailed analysis of DNA methylation levels of selected post-stasis HMEC-specific DMRs by MALDI-TOF. The rows show the gene promoters analyzed and the columns show each sample analyzed. The pie charts show the methylation status of each gene promoter for each HMEC sample (passage number is in parenthesis); the black region shows the average percent methylation of the entire region. Percent methylation of individual CpG sites is provided in Supplementary Figure 6.

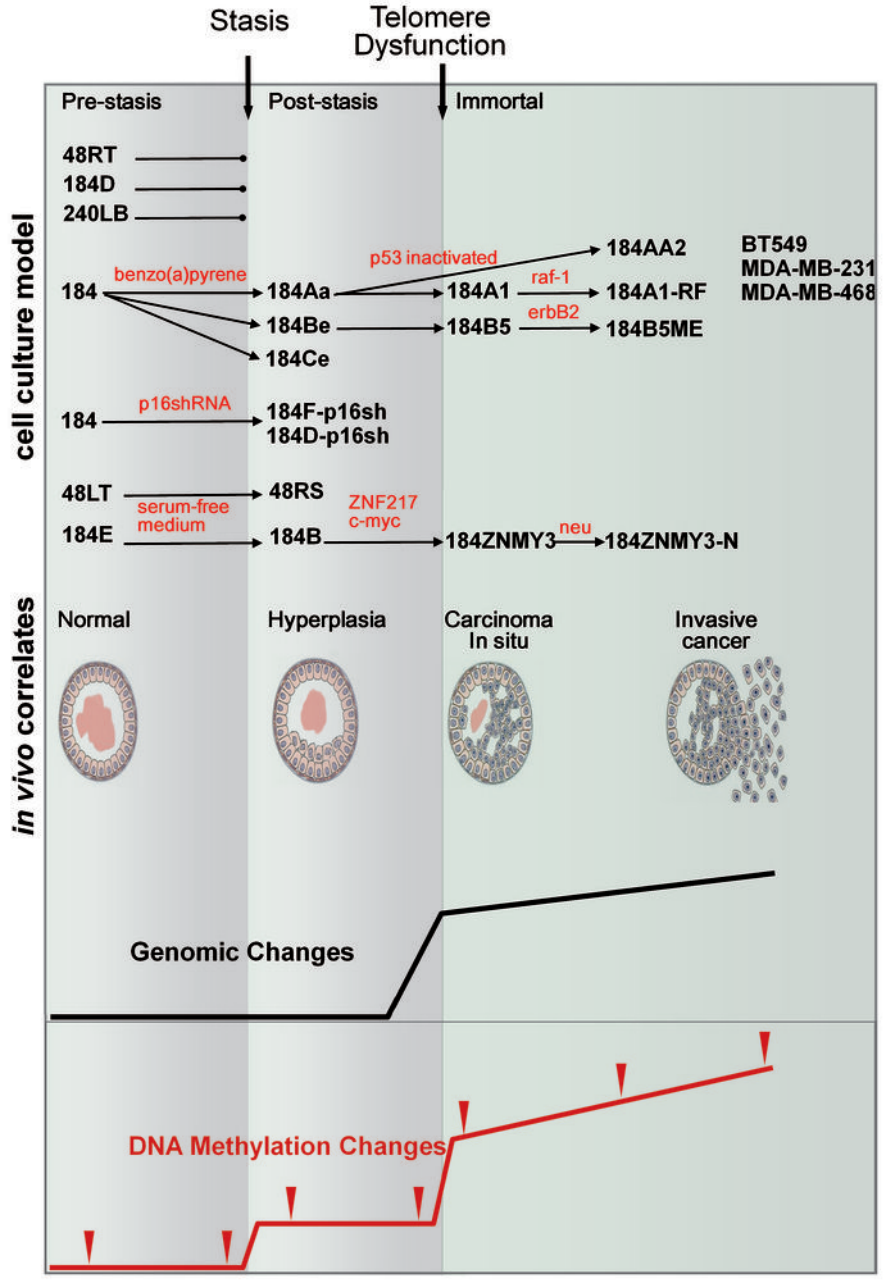
Stasis
Telomere Dysfunction
Pre-stasis
Post-stasis
Immortal
cell culture model
48RT
184D
240LB
184
benzo(a)pyrene
184Aa
184Be
184Ce
p53 inactivated
184AA2
184A1
raf-1
184A1-RF
184B5
erbB2
184B5ME
BT549
MDA-MB-231
MDA-MB-468
184
p16shRNA
184F-p16sh
184D-p16sh
48LT
serum-free medium
48RS
184E
184B
ZNF217
c-myc
184ZNMY3
neu
184ZNMY3-N
in vivo correlates
Normal
Hyperplasia
Carcinoma In situ
Invasive cancer
Genomic Changes
DNA Methylation Changes

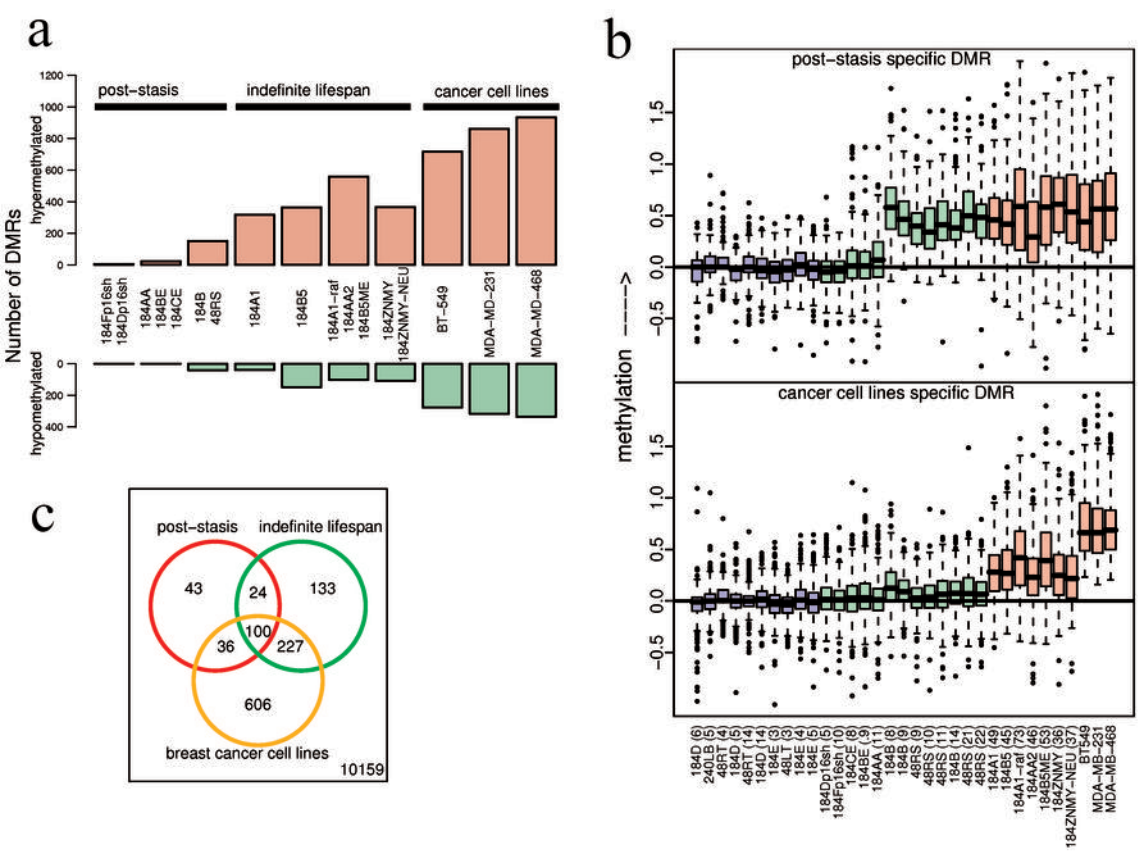
a
post−stasis
indefinite lifespan
cancer cell lines
Number of DMRs
hypermethylated
hypomethylated
1200
1000
800
600
400
200
0
184Fp16sh
184Dp16sh
184AA
184BE
184CE
184B
48RS
184A1
184B5
184A1−raf
184AA2
184B5ME
184ZNMY
184ZNMY−NEU
BT−549
MDA−MD−231
MDA−MD−468
b
post−stasis specific DMR
cancer cell lines specific DMR
methylation ----->
1.5
1.0
0.5
0.0
−0.5
184D (6)
240LB (5)
48RT (4)
184D (5)
48RT (14)
184D (14)
184E (3)
48LT (3)
184E (4)
184E (5)
184Dp16sh (10)
184Fp16sh (10)
184CE (8)
184BE (9)
184AA (11)
184B (8)
184B (9)
48RS (9)
48RS (10)
48RS (11)
184B (14)
48RS (21)
184A1 (22)
184A1 (42)
184B5 (45)
184A1−raf (73)
184AA2 (46)
184B5ME (53)
184ZNMY (36)
184ZNMY−NEU (37)
BT549
MDA−MB−231
MDA−MB−468
c
post−stasis
indefinite lifespan
breast cancer cell lines
43
24
133
100
36
227
606
10159

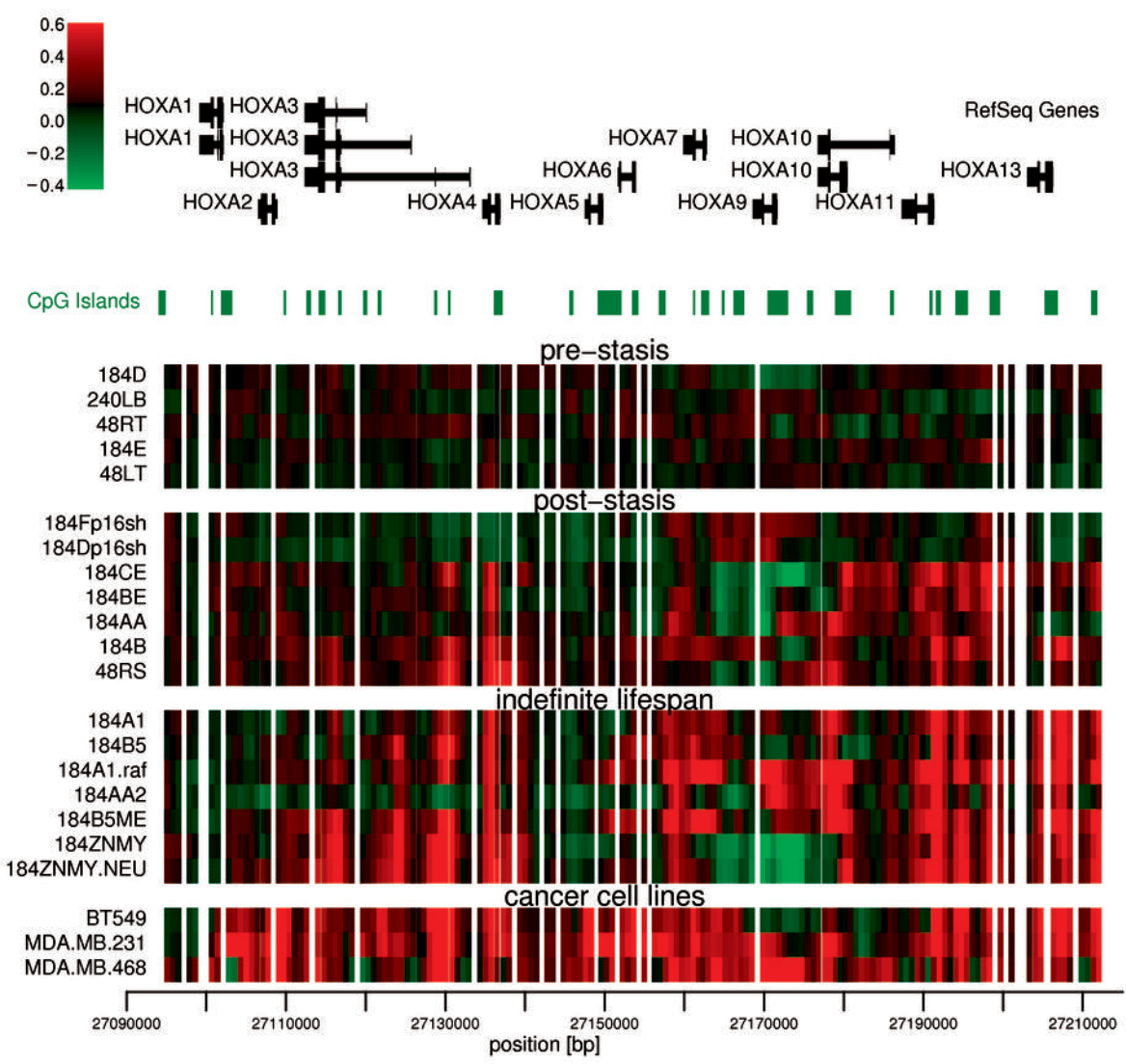
0.6
0.4
0.2
0.0
−0.2
−0.4
HOXA1
HOXA1
HOXA3
HOXA3
HOXA3
HOXA2
HOXA4
HOXA6
HOXA5
HOXA7
HOXA9
HOXA10
HOXA10
HOXA11
HOXA13
RefSeq Genes
CpG Islands
pre−stasis
184D
240LB
48RT
184E
48LT
post−stasis
184Fp16sh
184Dp16sh
184CE
184BE
184AA
184B
48RS
indefinite lifespan
184A1
184B5
184A1.raf
184AA2
184B5ME
184ZNMY
184ZNMY.NEU
cancer cell lines
BT549
MDA.MB.231
MDA.MB.468
27090000
27110000
27130000
27150000
27170000
27190000
27210000
position [bp]

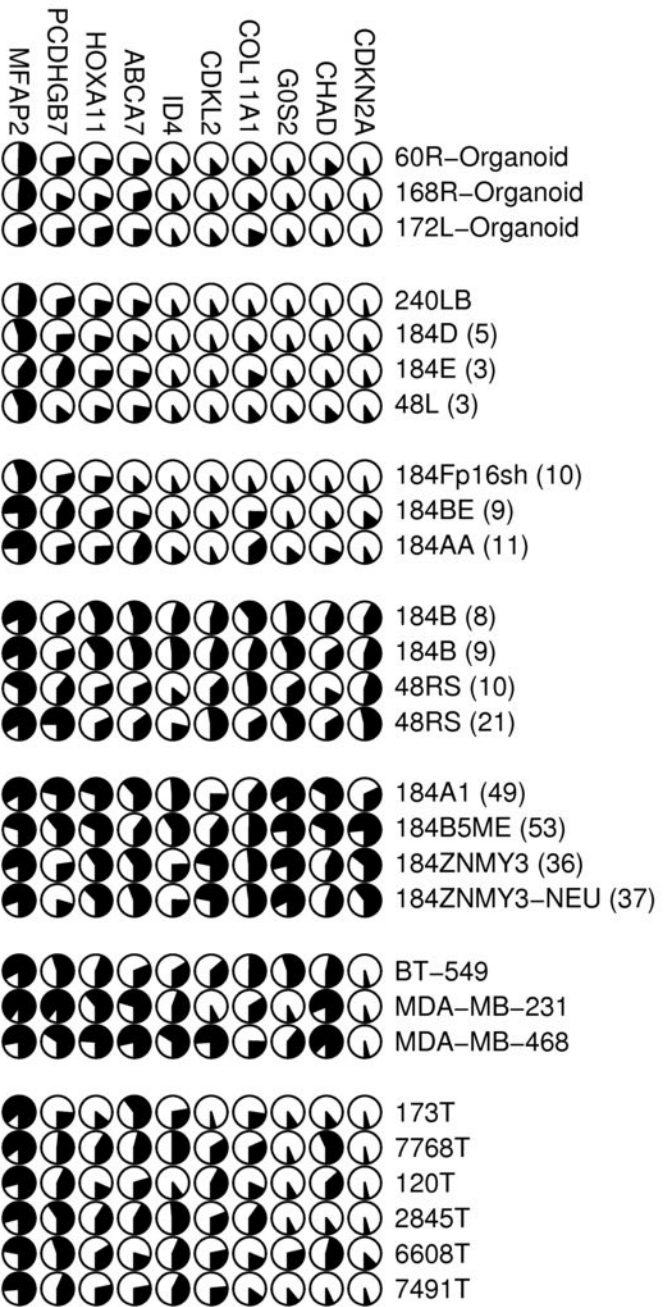
MFAP2
PCDHGB7
HOXA11
ABCA7
ID4
CDKL2
COL11A1
G0S2
CHAD
CDKN2A
60R–Organoid
168R–Organoid
172L–Organoid
240LB
184D (5)
184E (3)
48L (3)
184Fp16sh (10)
184BE (9)
184AA (11)
184B (8)
184B (9)
48RS (10)
48RS (21)
184A1 (49)
184B5ME (53)
184ZNMY3 (36)
184ZNMY3–NEU (37)
BT–549
MDA–MB–231
MDA–MB–468
173T
7768T
120T
2845T
6608T
7491T

Acknowledgments
Received 12/31/08; revised 3/27/09; accepted 4/20/09; published OnlineFirst 6/9/09.
Grant support: Grants R01CA65662 and R33CA091351 (B.W. Futscher); center grants P30ES06694 and P30CA023074 and the BIO5 Interdisciplinary Biotechnology Center at the University of Arizona (Genomics Shared Service); training grants ES007091 and CA09213(T. J. Jensen); and NIH grant U54 CA112970, Department of Defense grant BCRP BC060444, and Office of Energy Research, Office of Health and Biological Research, U.S. Department of Energy contract DE-AC02-05CH11231 (J.C. Garbe and M.R. Stampfer).
The costs of publication of this article were defrayed in part by the payment of page charges. This article must therefore be hereby marked advertisement in accordance with 18 U.S.C. Section 1734 solely to indicate this fact. We thank Jose Munoz-Rodriguez (University of Arizona) and Batul Merchant (Lawrence Berkeley National Laboratory) for outstanding technical support.